Reactivity and physicochemical properties of the soot produced in the pyrolysis of 2,5-dimethylfuran and 2-methylfuran

Katiuska Alexandrino[a,b]*, Ángela Millera[b], Rafael Bilbao[b], María U. Alzueta[b]*

[a] Grupo de Biodiversidad Medio Ambiente y Salud (BIOMAS), Universidad de Las Américas, calle José Queri y Av. de los Granados / Bloque 7, Quito – EC 170137 Ecuador

[b] Aragón Institute of Engineering Research (I3A). Department of Chemical and Environmental Engineering. University of Zaragoza. C/ Mariano Esquillor, s/n. 50018 Zaragoza. Spain

Corresponding authors:

Katiuska Alexandrino: katiuska.alexandrino@udla.edu.ec; katyalex@unizar.es

+593 23981000. Extension: 7830

M.U. Alzueta: uxue@unizar.es

+34 976761876

Abstract

Alkylated furan derivatives, such as 2,5-dimethylfuran (2,5-DMF) and 2-methylfuran (2-MF), have shown, at laboratory scale, a relatively high tendency to form soot. However, soot emissions from diesel engines are lower when diesel/2,5-DMF and diesel/2-MF blends are used. This could indicate that the soot produced in the conversion of these compounds has high reactivity towards some gases present within the combustion chamber, reducing soot emissions in the exhaust gas. In this context, a study on the reactivity and the characterization of the soot generated in the pyrolysis of 2,5-DMF and 2-MF, under different experimental conditions, was performed in an effort to increase the understanding of the reactivity and physicochemical properties of the soot originated in the conversion of these furan derivatives. The soot samples analyzed were obtained in previous works using different concentrations of the alkylated furan derivatives (5000, 7500 and 15000 ppm of 2,5-DMF, and 9000 and 18000 ppm of 2-MF), and at different temperatures (1275, 1375 and 1475 K). The reactivity experiments were performed at 1275 K with 500 ppm of O_2 and 2000 ppm of NO, in a tubular quartz flow reactor. Different instrumental analysis techniques were employed to characterize the soot samples and to try to link the soot reactivity with its physicochemical properties. The dependence of soot reactivity and properties with soot formation conditions, namely temperature and inlet fuel concentration, is studied.

Keywords: 2,5-dimethylfuran, 2-methylfuran, soot, reactivity, characterization

1. Introduction

Diesel engines are known to be an important source of soot emissions due to the high working temperature and the poor mixing in the fuel-rich chamber areas. A possible strategy to control soot emissions requires the utilization of alternative fuels, such as biofuels obtained from biomass by biorefinery processes.

2,5-dimethylfuran (2,5-DMF, C_6H_8O) and 2-methylfuran (2-MF, C_5H_6O) are alkylated furan derivatives. These compounds have been proposed in the literature for fuel reformulation. Their conversion has been largely studied in engines and at laboratory-scale. Alexandrino et al.[1,2] studied the capacity to form soot of 2,5-DMF and 2-MF through pyrolysis experiments in a tubular flow reactor and found that these compounds have a relatively high sooting tendency. In the 2-MF pyrolysis[2], C4-species were found to play a significant role in the formation of intermediates that yield polycyclic aromatic hydrocarbons (PAH), well known as soot precursors. In the 2,5-DMF pyrolysis[1], the high production of cyclopentadienyl radical (C_5H_5) can directly form naphthalene. Moreover, Sirignano et al.[3] addressed the sooting tendency of furans by laser induced incandescense (LII) and laser induced fluorescence (LIF). Their results indicated that 2-MF had a greater capacity to originate soot particles than 2,5-DMF, although different combustion conditions may invert this trend. They also found that the 2-MF decomposition leads to the formation of large amounts of C4-species, which consequently increases the production of benzene and PAH. In the same way, they indicated that one of the main products of the decomposition of 2,5-DMF is phenol, which increases the production of cyclopentadiene and, therefore, the naphthalene formation.

These results, together with others obtained in several works[4-9], point out 2,5-DMF and 2-MF as non-environment-friendly renewable fuels due to their relatively high abilities to form soot precursors. Nevertheless, the use of these alkylated furan derivatives in diesel fuel blends has been shown to effectively reduce particulate matter[10-13]. These works were performed in

engines with diesel/2,5-DMF or diesel/2-MF blends, and the authors often state that the low cetane number of these fuels is the most important factor in reducing soot emissions, because it lengthens the ignition delay time, which results in a greater premixed combustion. Moreover, the capacity of these furans to reduce soot formation has also been verified at laboratory-scale, in the study carried out by Sirignano et al.[14] on the conversion of 2,5-DMF and 2-MF in premixed ethylene-air flames at atmospheric pressure.

These apparently contradictory facts (high ability of the furan compounds to form soot precursors and capacity to reduce soot emissions) can also be related to physical and chemical properties of soot that may favour its reactivity. In fact, a recent study carried out in a diffusion flame[15] showed that the use of diesel/2,5-DMF blends reduced soot emissions and increased the reactivity of soot particles towards O_2.

In this context, it is important to study the soot reactivity with gases present in the combustion chamber of an engine, as for example O_2 and NO. The reactivity of soot with NO is of special interest, since both pollutants could be reduced simultaneously within the combustion chamber, and their emissions in the exhaust gases could decrease. Therefore, this work addresses the experimental reactivity study towards O_2 and NO of soot samples obtained in our previous studies on the pyrolysis of 2,5-DMF[1] and 2-MF[2] under different inlet fuel concentration and temperature conditions. Moreover, different instrumental techniques have been used in order to characterize selected soot samples, because several works performed, both at laboratory scale[15-20] and in engines[21-26], have shown that the soot oxidation rate depends on its properties. In this way, the aim of this work is to provide information on the reactivity and physicochemical properties of the soot produced in the conversion of these alkylated furan derivatives.

2. Material and methods

2.1. Soot formation and collection

The soot samples were obtained in our previous works on the pyrolysis of 2,5-DMF[1] and 2-MF[2]. The reaction system consists of an injection zone, into which the gases are fed, and a tubular quartz flow reactor, with a mobile probe that allows us to determine the volume of the reaction zone. In the experiments corresponding to this work, the reaction zone has a diameter of 45 mm and its length is 160 mm. The inlet total gas volumetric flow rate is 1 L (STP)/min. Therefore, the gas residence time is given as t_r (s) = 4168/T (K). The soot produced in each experiment was collected using a quartz fiber filter, with a pore diameter lower than 1 μm, located at the outlet of the reaction system. The soot amount collected in the filter (soot A) was obtained by the difference between the weight of the filter after and before the soot collection. Furthermore, when each experiment finished, the soot that remained on the walls of the reactor was also recovered (soot B). Thereby, the total amount of soot was the sum of soot A and soot B. Table 1 shows the experimental conditions employed in the formation of the soot samples for which reactivity experiments and characterization were performed. The corresponding nomenclature is also shown.

Table 1. Conditions of formation of soot samples for the reactivity study towards O_2 and NO and for their characterization. "X" indicates the soot samples used for the reactivity experiments and characterization.

Furan compound	Set	Nomenclature	Soot formation conditions			Reactivity	Characterization
			[Furan compound]$_{in}$ (ppm)	[Carbon]$_{in}$ (ppm)	T (K)		
2,5-DMF	1	2,5DMF5-1275			1275	X	X
	2	2,5DMF5-1375	5000	30000	1375	X	
	3	2,5DMF5-1475			1475	X	
	4	2,5DMF7-1275			1275	X	X
	5	2,5DMF7-1375	7500	45000	1375	X	
	6	2,5DMF7-1475			1475	X	
	7	2,5DMF15-1275			1275	X	X
	8	2,5DMF15-1375	15000	90000	1375	X	X
	9	2,5DMF15-1475			1475	X	X
2-MF	10	2MF9-1275			1275	X	
	11	2MF9-1375	9000	45000	1375	X	
	12	2MF9-1475			1475	X	
	13	2MF18-1275			1275	X	X
	14	2MF18-1375	18000	90000	1375	X	X
	15	2MF18-1475			1475	X	X

2.2. Soot reactivity

The soot reactivity measurements, towards O_2 and NO, have been carried out in a set-up that has been used in previous works[27-29]. Schemes of the set-up and the reactor are presented in the supplementary material, Figure S1. The process is discontinuous for the solid and continuous for the gas. Briefly, the soot sample was mixed with silica sand and introduced in a tubular quartz reactor. The concentrations of both O_2 and NO were 500 and 2000 ppm respectively, as used in previous works of our group[16,30]. The reaction temperature and the gas volumetric flow rate were 1275 K and 1 L (STP)/min, respectively. The concentrations of CO, CO_2, and NO, the latter when applicable, were continuously analyzed in the output gas stream using ABB infrared analysers (uncertainty measurements below ±5%).

Previously to perform the reactivity experiments and characterization, the soot samples were conditioned by heating treatment for one hour in a N_2 atmosphere, at the soot formation temperature to avoid possible structural changes[30].

The carbon complete conversion time (τ) value is used to analyze the soot reactivity. Thus, the lower the τ value, the higher the soot reactivity. The τ values are determined through Eq. 1, which relates the carbon conversion (X_c) and reaction time (t). In this way, τ value is calculated as the reverse of the slope obtained from the representation of the $1-(1-X_C)^{1/3}$ values versus the corresponding reaction time values.

$$1-(1-X_C)^{1/3}=\frac{t}{\tau} \qquad \text{Eq. 1}$$

This equation corresponds to a non-catalytic gas-solid reaction using Shrinking Core Model for decreasing size particles and chemical reaction control and has already been used in previous soot reactivity studies[16, 31-33].

The carbon conversion is calculated using the following equations[31-33]:

$$X_c=\frac{(W_{c0}-W_c)}{W_{c0}} \qquad \text{Eq. 2}$$

$$W_{c0}=10^{-3}M_cF_T\int_0^{\infty}(C_{CO}+C_{CO_2})dt \qquad \text{Eq. 3}$$

$$W_c=W_{c0}-10^{-3}M_cF_T\int_0^{t}(C_{CO}+C_{CO_2})dt \qquad \text{Eq. 4}$$

Where, W_{c0}: initial reactive carbon weight (mg), W_c: carbon weight remaining in the reactor at a given time (mg), C_{CO} and C_{CO_2} : CO and CO_2 concentrations (ppm) at the reactor outlet, respectively, M_c: carbon atomic weight (g/mol), F_T: outlet gas flow (mol/s).

The carbon conversion results versus reaction time ($X_c=f(t)$) are presented in the supplementary material (Figures S2 and S3).

The experimental procedure followed to perform the experiments, as well as the data analysis method for the calculation of the τ value, have been applied in similar earlier studies[e.g.16, 31-33]. In the present work, the relative standard deviation (RSD) values, also known as coefficient of variation (CV), and defined as the ratio of the standard deviation to the mean value, are shown here for given experiments. For reactivity tests with NO for soot samples appointed as 2,5-DMF5-1475 and 2,5-DMF7-1475 in Table 1, the results obtained have been:

- Soot sample 2,5-DMF5-1475. τ values: 17903 s and 18228 s, standard deviation: 229.8 s, mean value: 18065 s , relative standard deviation or coefficient of variation: 1.3 %.
- Soot sample 2,5-DMF7-1375. τ values: 16296 s and 17000 s, standard deviation: 497.8 s, mean value: 16648 s , relative standard deviation or coefficient of variation: 3 %.

2.3. Physicochemical characterization of soot

The characterization of soot by different instrumental techniques presents a clear interest, since it can provide information on the relationship between soot reactivity and its properties. Thus, elemental analysis (composition), nitrogen physical adsorption (surface area), Transmission Electron Microscopy (TEM) (morphology), X-Ray Diffraction (XRD) (crystallite structure), and Raman spectroscopy (degree of order) have been employed to characterize selected soot samples. The selected soot samples characterized are indicated in Table 1.

3. Results and discussion

3.1. Soot reactivity

Figure 1 shows the τ values, in seconds, obtained in the experiments of interaction of soot with O_2 and NO at 1275 K, for soot samples produced in the pyrolysis of different inlet fuel concentrations and temperatures. A Table with all the τ values is also presented in the

supplementary material (Table S1). It is noted that the soot reactivity is higher with O_2 than with NO, although the oxygen content in NO is higher than in O_2 (2000 vs. 1000 ppm of oxygen atoms). This result coincides with those from literature[27, 30, 34, 35].

It is observed that, for a given furan compound and a fixed inlet concentration, the higher the soot formation temperature, the lower the soot reactivity (τ value increases). Moreover, for a fixed temperature, the inlet concentration of the furan compound does not significantly influence the soot reactivity, except for the soot produced in the pyrolysis of 5000 ppm of 2,5-DMF at 1275 K. In this case, the reactivity towards O_2 and NO is slightly higher (τ value is lower), with respect to other furan concentrations.

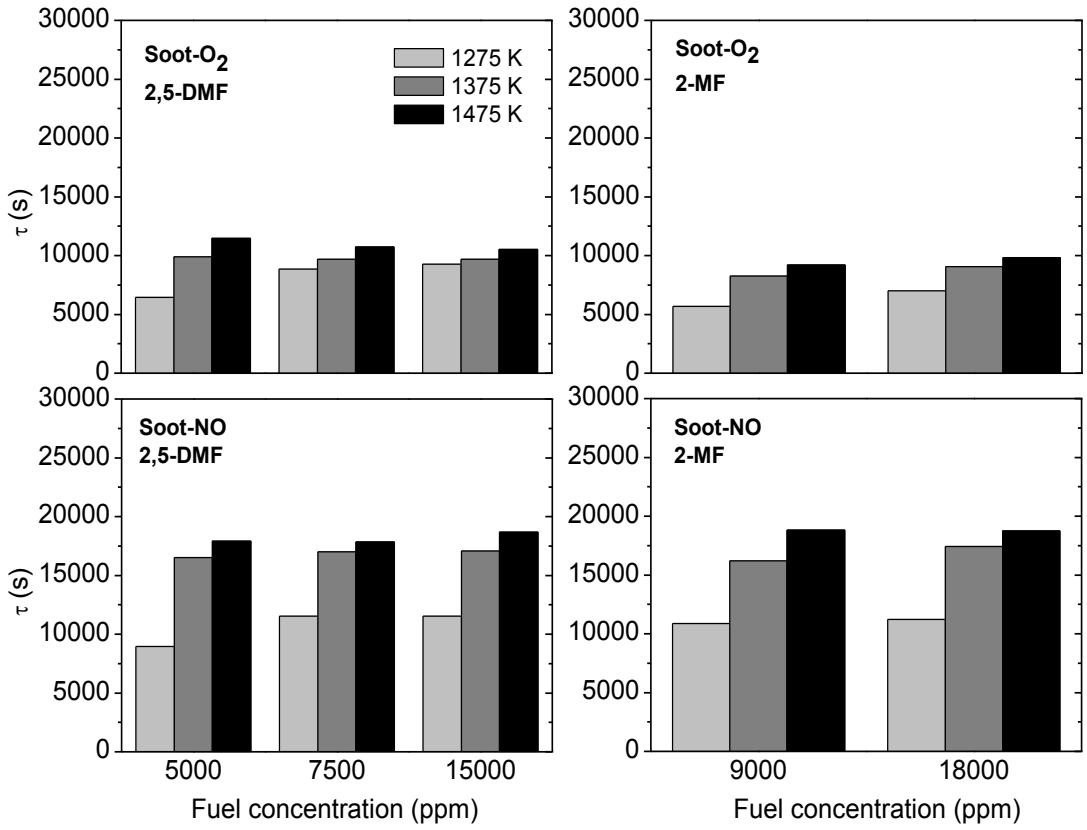

Figure 1. τ values (s) obtained in the reactivity experiments towards O_2 and NO at 1275 K, for samples of sets 1-15 in Table 1.

A comparison between the τ values obtained, both with O_2 and NO, for the soot samples formed from pyrolysis of the two furan derivatives and selected for characterization (sets 7-9, 13-15 in Table 1) versus soot formation temperature is presented in Figure 2. For a given temperature, the τ values obtained in the reactivity experiments with NO are very similar for the two compounds (around 11300 s for 1275 K, 17200 s for 1375 K, 18700 s for 1475 K), which confirms that the most influential variable is the soot formation temperature. Similar conclusions are obtained for the reactivity with O_2 for 1375 and 1475 K (around 9300 and 10000 s, respectively). The exception is for 1275 K, with significant differences in the τ values (9285 s for 2,5-DMF and 6996 s for 2-MF).

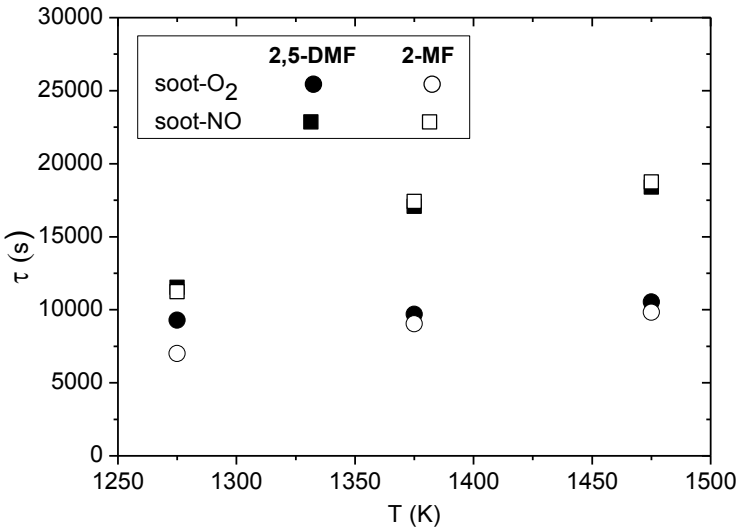

Figure 2. τ values versus soot formation temperature (Sets 7-9, 13-15 in Table 1).

It is worth mentioning that the soot samples produced in the pyrolysis of 2,5-DMF and 2-MF are more reactive (lower τ value) than the soot samples produced in the pyrolysis of other oxygenated compounds with low tendency to form soot, such as DMC[32] and DMM[33]. This fact is clear for the soot-NO interaction. Hence, it is possible that, although 2,5-DMF and 2-MF have a relatively high tendency to form soot, this soot could have properties that favour its reactivity, as it has been pointed out in the literature. For instance, Gogoi et al.[15] in their study

on diffusion flame of diesel and diesel/2,5-DMF blends, indicated that the soot produced from diesel/2,5-DMF blends could be oxidized more rapidly in the bulk gas, and then, soot emissions would be lower. The same could be applied for 2-MF.

3.2. Physicochemical characterization of soot

Elemental analysis

Table 2 presents the results of the elemental analyses performed. Carbon is the principal component of soot. The atomic ratio of carbon to hydrogen (C/H) can be used to analyze the material reactivity[1,2]. For a fixed inlet fuel concentration, the lower the soot formation temperature, the lower the C/H ratio (lower maturity, and the reactivity could be promoted). This trend is consistent with reactivity measurements (Figure 1 and Table S1), where the lower the soot formation temperature, the greater the soot reactivity (the τ values decrease). On the other hand, at a fixed temperature, there is no clear trend between the C/H ratio and the inlet fuel concentration.

Table 2. Content of C and H, and C/H ratio of the soot samples.

Furan compound	Set according to Table 1	Sample	C (wt%)	H (wt%)	C/H (molar basis)
2,5-DMF	1	2,5DMF5-1275	93.18	0.27	28.76
	4	2,5DMF7-1275	96.91	0.18	44.87
	7	2,5DMF15-1275	98.39	0.23	35.65
	8	2,5DMF15-1375	98.63	0.12	68.49
	9	2,5DMF15-1475	98.01	0.09	90.75
2-MF	13	2MF18-1275	95.08	0.27	29.35
	14	2MF18-1375	99.00	0.09	91.67
	15	2MF18-1475	98.96	0.06	137.44

Nitrogen physical adsorption

Specific surface area (S_{BET}) of the soot samples was determined by nitrogen physical adsorption. Large specific surface area improves the contact between the gas oxidizer molecule and the particle promoting the oxidation reactions[36-38]. The results are reported in

Table 3. The soot samples with the highest specific surface area are those from the pyrolysis at 1275 K of 2,5-DMF and 2-MF (samples 2,5DMF5-1275, 2,5DMF7-1275, 2,5DMF15-1275, and 2MF18-1275). In this way, the S_{BET} values are in accordance with the trend of the reactivity experiments, i.e., for a given fuel, the soot samples produced at the lowest temperature and with the lowest inlet fuel concentration are more reactive.

Table 3. Specific surface area (S_{BET}) of the soot samples produced in the pyrolysis of 2,5-DMF and 2-MF.

Furan Compound	**Set according to Table 1**	**Sample**	**S_{BET} (m^2/g)**
2,5-DMF	1	2,5DMF5-1275	128.2
	4	2,5DMF7-1275	66.7
	7	2,5DMF15-1275	60.2
	8	2,5DMF15-1375	30.7
	9	2,5DMF15-1475	33.3
2-MF	13	2MF18-1275	110.9
	14	2MF18-1375	35.3
	15	2MF18-1475	38.3

The comparison between the S_{BET} values obtained for the soot samples, formed from the pyrolysis of the two compounds, versus soot formation temperature is presented in Figure 3. For a given temperature, the S_{BET} values are very similar for both compounds, except for 1275 K, being higher the value corresponding to 2-MF, which causes its higher reactivity at this temperature (see Figure 2).

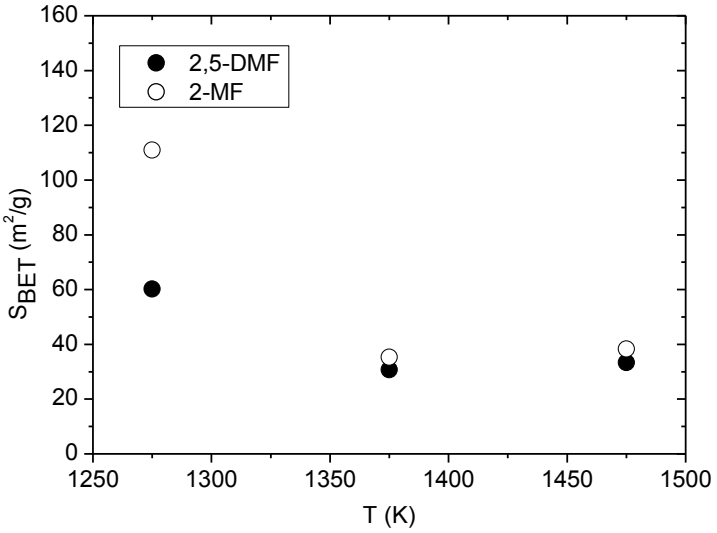

Figure 3. Specific surface area (S_{BET}) of the soot samples versus soot formation temperature (Sets 7-9, 13-15 in Table 1).

Transmission Electron Microscopy (TEM)

Through the TEM images, the diameters of the soot samples were determined, and they were found to be close to those of the secondary particles, 100-1000 nm. As an example, Figure 4 presents the TEM image of the 2,5DMF15-1475 soot sample (set 9 in Table 1).

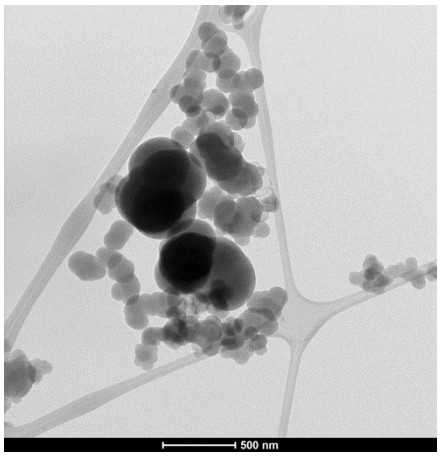

Figure 4. TEM image of the 2,5DMF15-1475 sample (set 9 in Table 1).

It is possible to observe the secondary particles that form the typical chain-like agglomerates. These secondary particles are formed by several primary particles composed of more or less ordered and amorphous domains.

X-Ray Diffraction (XRD)

Figure 5 shows, as an example, the X-ray diffractogram for the 2,5DMF15-1475 soot sample. The (002), (100) and (110) reflections of graphite are characterized by the peaks near 2θ = 24°, 2θ = 44° and 2θ = 80°, respectively. The background intensity indicates the presence of amorphous carbon (non-aromatic carbon)[39]. The asymmetry in the (002) band suggests the occurrence of another band (*γ*) around 2θ = 20°, which indicates the presence of saturated structures, such as aliphatic side chains, attached to the edge of the crystallites[16, 28, 40, 41]. Thus, it can be concluded that the soot samples contain crystalline and amorphous carbon[40].

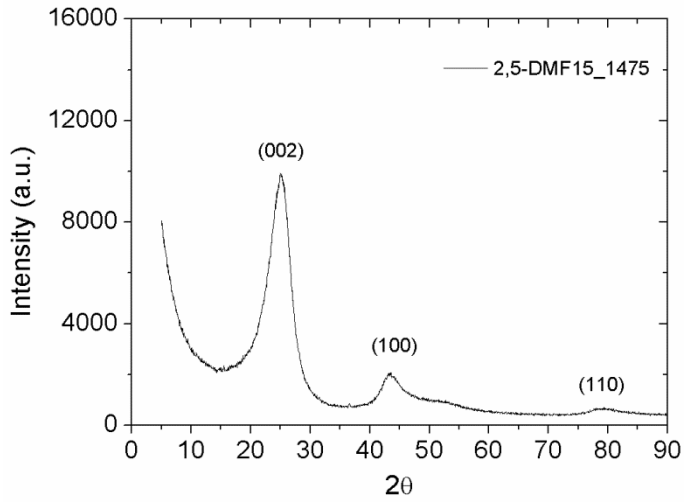

Figure 5. X-ray diffractogram of the 2,5DMF15-1475 sample (set 9 in Table 1).

Table 4 shows the values of the most important structural parameters of interest determined from the X-ray diffractogram, such as the interlayer spacing (d_{002}), the crystallite height (L_c) and width (L_a), and the number of layers in a crystallite (k) (see references 32 and 33 for details in

the calculations). Table 4 also reports the aromaticity of soot samples, f_a, which can be calculated according to Eq. 5.

$$f_a = \frac{A_{(002)}}{A_{(002)} + A_{(\gamma)}} \qquad \text{Eq. 5}$$

$A_{(002)}$ is the area under the (002) band, and is equal to the number of aromatic carbon atoms per structure unit, and $A_{(\gamma)}$ is the area under the (γ) band, and is equal to the number of saturated carbon atoms per structure unit[41]. To determine the values of $A_{(002)}$ and $A_{(\gamma)}$, both (002) and (γ) bands were fitted with two Gaussian functions.

Table 4. Structural parameters of the crystalline structure of the soot samples.

Furan compound	Set according to Table 1	Sample	d_{002} (Å)	L_c (Å)	L_a (Å)	k (layers)	f_a
2,5-DMF	1	2,5DMF5-1275	3.60	14.29	44.12	3.97	0.84
	4	2,5DMF7-1275	3.56	17.38	39.95	4.88	0.80
	7	2,5DMF15-1275	3.51	24.94	40.39	7.11	0.85
	8	2,5DMF15-1375	3.53	25.04	40.65	7.09	0.78
	9	2,5DMF15-1475	3.53	25.40	49.46	7.19	0.80
2-MF	13	2MF18-1275	3.63	14.14	30.50	3.90	0.89
	14	2MF18-1375	3.54	23.30	42.50	6.59	0.72
	15	2MF18-1475	3.52	27.62	47.91	7.84	0.76

It is observed in Table 4 that for all soot samples, the d_{002} value is higher than 3.35 Å, which is the value corresponding to pure graphite. This suggests that there is a lower order due to the weaker forces of attraction between the carbon layers. The L_C value is known to be directly related to the degree of order[42]. Therefore, it can be noted that as the soot formation temperature increases, the degree of order increases and, then, the soot reactivity decreases. This is in agreement with what is observed in reactivity experiments (Figure 1 and Table S1). In the same way, for a fixed soot formation temperature of 1275 K, the lowest L_C value

corresponds to the soot obtained with the lowest inlet fuel concentration. This is also consistent because this soot has a higher reactivity.

It is known that the soot reactivity decreases as the L_a value increases[43]. Observing Table 4, the trend of the L_a values, with respect to the soot formation temperature, coincides with the reactivity trend. The number of layers in a crystallite (k) seems to decrease with the decrease in temperature and inlet fuel concentration.

With respect to the aromaticity, the more aromatic (higher f_a value), the less reactive is the material[16]. There is no clear trend between the f_a value in Table 4 and the soot formation conditions.

The values of L_C and L_a corresponding to the soot samples from the pyrolysis of 2,5-DMF and 2-MF versus soot formation temperature are compared in Figure 6. For a given temperature, in general, these values are very similar for the two compounds except for 1275 K, being lower the values corresponding to 2-MF, which is related to a higher reactivity.

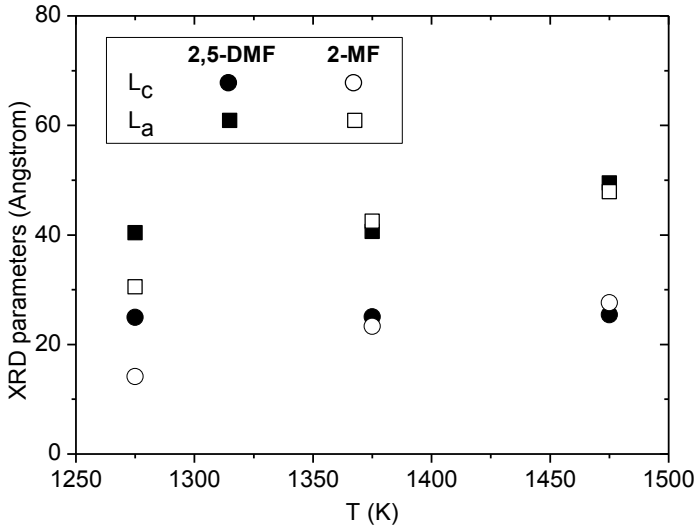

Figure 6. Crystallite height (L_C) and width (L_a) of the soot samples versus soot formation temperature (Sets 7-9, 13-15 in Table 1).

It has also been considered interesting to relate the τ values with L_C and L_a ones (Figures 7). Relatively good correlations are obtained for the soot samples produced from both furan compounds, except the results corresponding to the reactivity with NO of the soot formed from the 2,5-DMF pyrolysis at 1275 K.

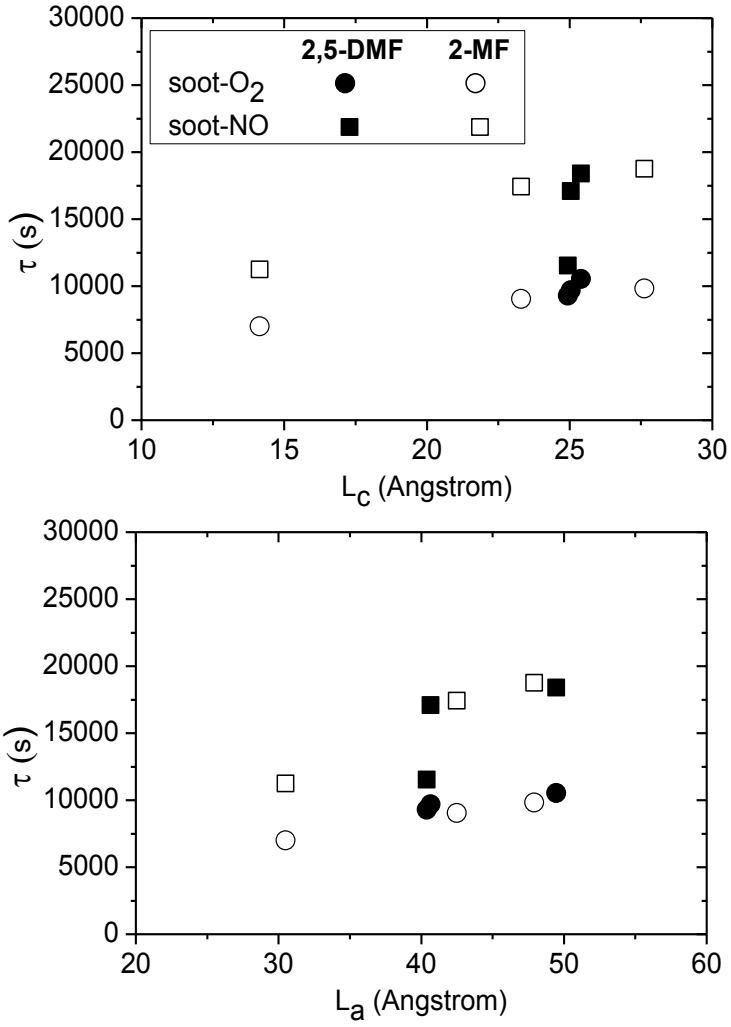

Figure 7. τ values versus crystallite height (L_C) and width (L_a) of the soot samples (Sets 7-9, 13-15 in Table 1).

Raman spectroscopy

The five-curve deconvolution model proposed by Sadezky et al.[44] has been employed in the present work in order to determine the bandwidth (FWHM), band intensity, and peak position

of the bands G, D1, D2, D3, and D4. All these bands, except D3, have been modeled by a Lorentzian band shape. A Gaussian band shape has been used for the D3 band [43, 45-49]. Figure 8 shows, as an example, the band deconvolution of the Raman spectrum of the 2,5DMF15-1475 soot sample.

Table 5 shows the presence of the defects (disordered graphitic lattices), calculated from the I_{D1}/I_G ratio, and the amorphous carbon content in soot particles, calculated from the I_{D3}/I_G ratio[22, 50, 51]. In general, for a fixed inlet concentration of a given fuel, the lower the soot formation temperature, the higher the I_{D1}/I_G and I_{D3}/I_G ratios. This means that the order is lower and the amorphous character is higher (i.e. the reactivity increases) as the soot temperature formation decreases, which is consistent with the reactivity results (Figure 1 and Table S1). This is in agreement with what is observed in literature[50], related to the fact that the lower the combustion temperature at which soot is formed, the lower the degree of graphitization, and, consequently, the higher the active surface available for further oxidation.

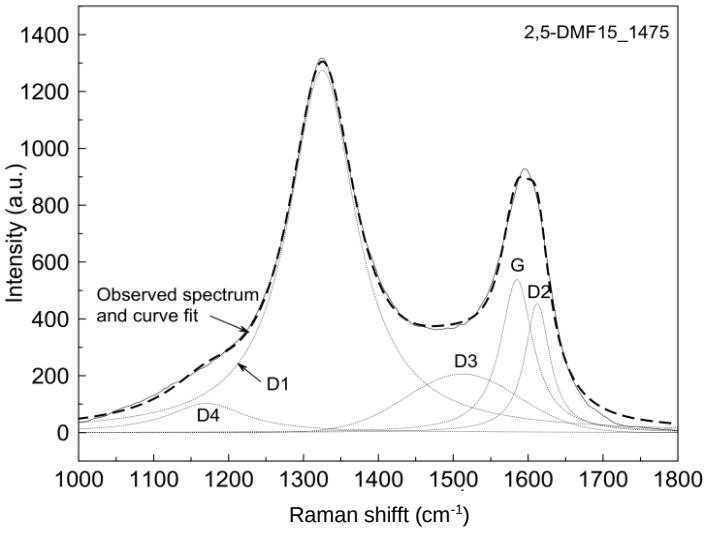

Figure 8. First-order Raman spectrum of the 2,5DMF15-1475 soot sample (set 9 in Table 1) with the five-curve deconvolution model proposed by Sadezky et al.[44]

Table 5. I_{D1}/I_G and I_{D3}/I_G ratio values of the soot samples.

Furan compound	Set according to Table 1	Sample	I_{D1}/I_G	I_{D3}/I_G
2,5-DMF	1	2,5DMF5-1275	2.58	0.64
	4	2,5DMF7-1275	2.64	0.71
	7	2,5DMF15-1275	2.70	0.65
	8	2,5DMF15-1375	2.48	0.65
	9	2,5DMF15-1475	2.37	0.38
2-MF	13	2MF18-1275	2.56	0.64
	14	2MF18-1375	2.34	0.64
	15	2MF18-1475	2.22	0.40

The values of I_{D1}/I_G and I_{D3}/I_G corresponding to the soot samples formed from 2,5-DMF and 2-MF for different soot formation temperatures are compared in Figure 9. Again, for a given temperature, the values are very similar for both furan derivatives.

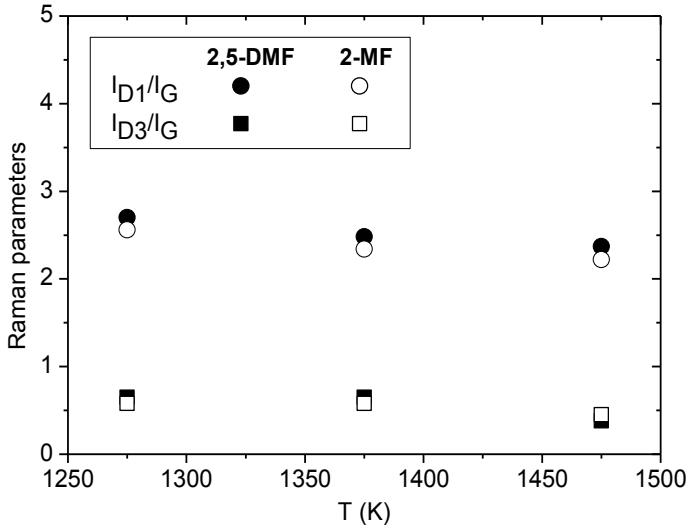

Figure 9. ID_1/IG and ID_3/IG values of the soot samples versus soot formation temperature (Sets 7-9, 13-15 in Table 1).

It has also been considered interesting to relate the τ values with the values of I_{D1}/I_G and I_{D3}/I_G corresponding to the soot samples produced from both compounds, Figure 10. In general, a

relatively good correlation is obtained for I_{D1}/I_G values, while more dispersion is obtained for I_{D3}/I_G values.

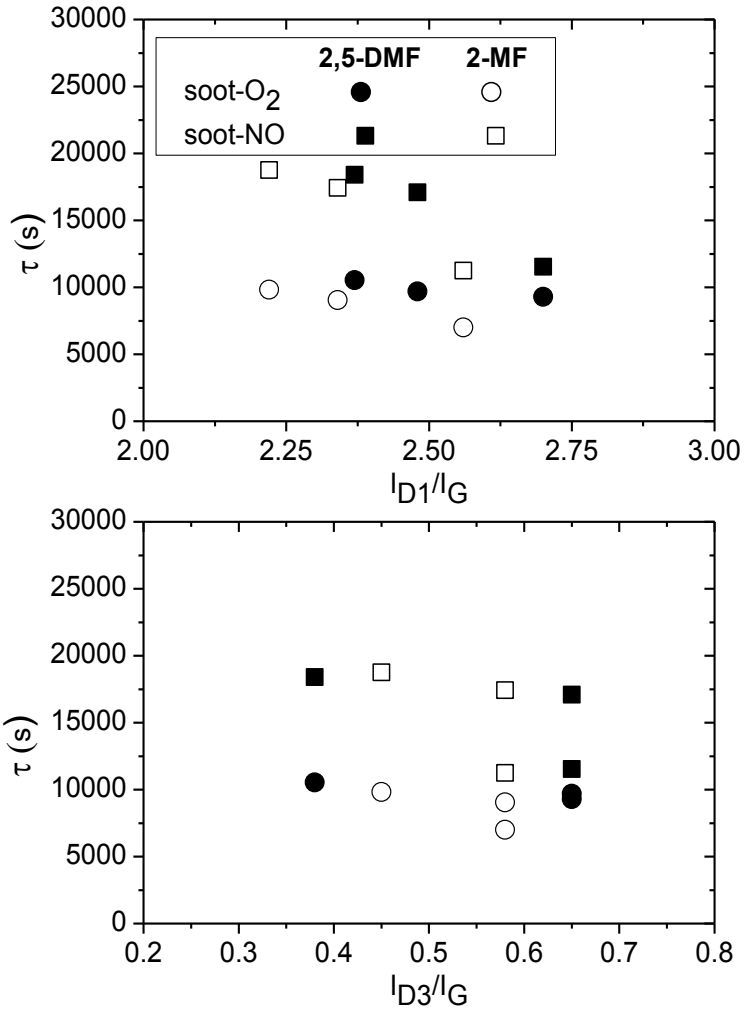

Figure 10. τ values versus I_{D1}/I_G and I_{D3}/I_G values of the soot samples (Sets 7-9, 13-15 in Table 1).

4. Conclusions

A study on the reactivity, towards O_2 and NO, of soot samples produced in the pyrolysis of 2,5-DMF and 2-MF under different experimental conditions, was performed in a tubular quartz flow reactor at 1275 K. Additionally, in order to link the reactive character of the soot samples with their physicochemical properties, selected soot samples were analyzed using different instrumental techniques.

According to the reactivity experiments, soot is more reactive to O_2 than to NO, being more reactive as the temperature of the soot formation decreases. In general, no appreciable effect of the inlet fuel concentration was found on the soot reactivity. An exception was observed for the soot produced in the pyrolysis of the lowest 2,5-DMF concentration and temperature (5000 ppm and 1275 K) for which the highest reactivity was obtained. This soot sample presents the lowest C/H ratio, the highest specific surface area, the lowest L_C and L_a values (obtained by XRD) and significant I_{D1}/I_G and I_{D3}/I_G values (obtained by Raman spectroscopy). These features are consistent with the higher reactivity of this soot sample. The physicochemical analyses showed that as lower the C/H ratio and the order degree are, and higher the surface area and the amorphous nature are, the more reactive the soot. In general, relatively good correlations are observed between the τ values and the soot characterization parameters. The soot samples from the pyrolysis of 2,5-DMF and 2-MF appear to have a higher reactive character than those from the pyrolysis of other oxygenated compounds with lower sooting tendency, such as dimethylcarbonate and dimethoxymethane, especially towards NO.

Acknowledgment

The authors acknowledge the financial support from the AragónGovernment (Ref. T22_17R), co-funded by FEDER 2014-2010 "*Construyendo Europa desde Aragón*", and MINECO and FEDER (Project CTQ2015-65226). Ms. K. Alexandrino acknowledges to MINECO the pre-doctoral grant awarded (BES-2013-063049).

References

(1) Alexandrino, K.; Salvo, P.; Millera, Á.; Bilbao, R.; Alzueta M.U. Influence of the temperature and 2,5-dimethylfuran concentration on its sooting tendency. Combust. Sci. Tech. **2016**, 188, 651–666.

(2) Alexandrino, K.; Baena, C.; Millera, Á.; Bilbao, R.; Alzueta M.U. 2-methylfuran pyrolysis: gas-phase modelling and soot formation. Combust Flame **2018**, 188, 376–387.

(3) Sirignano, M.; Conturso, M.; D'Anna, A. Effect of furans on particle formation in diffusion flames: an experimental and modeling study. Proc. Combust. Inst. **2015**, 35, 525–532.

(4) Cheng, Z.; Xing, L.; Zeng, M.; Dong, W.; Zhang, F.; Qi, F.; Li, Y. Experimental and kinetic modeling study of 2,5-dimethylfuran pyrolysis at various pressures. Combust. Flame **2014,** 161, 2496–2511.

(5) Djokic, M.; Carstensen, H.; Van Geem, K.M.; Marin, G.B. The thermal decomposition of 2,5-dimethylfuran. Proc. Combust. Inst. **2013**, 34, 251–258.

(6) Togbé, C.; Tran, L.-S.; Liu, D.; Felsman, D.; Oßwald, P.; Glaude, P.-A.; Sirjean, B.; Fournet, R.; Battin-Leclerc F.; Kohse-Höinghaus K. Combustion chemistry and flame structure of furan group biofuels using molecular-beam mass spectrometry and gas chromatography-Part III: 2,5-dimethylfuran. Combust. Flame **2014**, 161, 780–797.

(7) Tran, L.-S.; Sirjean B.; Glaude, P.A.; Kohse-Höinghaus, K.; Battin-Leclerc, F. Influence of substituted furans on the formation of polycyclic aromatic hydrocarbons in flames. Proc. Combust. Inst. **2015**, 35, 1735–1743.

(8) Moshammer, K.; Lucassen, A.; Togbé, C.; Kohse-Höinghaus, K.; Hansen, N. Formation of oxygenated and hydrocarbon intermediates in premixed combustion of 2-methylfuran. Zeitschrift für Physikalische Chemie **2015**, 229, 507–528.

(9) Cheng, Z.; He, S.; Xing, L.; Wei, L.; Li, W.; Li, T.; Yan, B.; Ma. W; Chen, G. Experimental and kinetic modeling study of 2-methylfuran pyrolysis at low and atmospheric pressures. Energy Fuels **2017**, 31, 896–903.

(10) Chen, G.; Shen, Y.; Zhang, Q.; Yao, M.; Zheng, Z.; Liu, H. Experimental study on combustion and emission characteristics of a diesel engine fueled with 2,5-dimethylfuran–diesel, n-butanol–diesel and gasoline-diesel blends. Energy **2013**, 54, 333–342.

(11) Liu, H.; Xu, J.; Zheng, Z.; Li, S.; Yao, M. Effects of fuel properties on combustion and emissions under both conventional and low temperature combustion mode fueling 2,5-dimethylfuran/diesel blends. Energy **2013**, 62, 215–223.

(12) Xiao, H.; Zeng, P.; Li, Z.; Zhao, L.; Fu, X. Combustion performance and emissions of 2-methylfuran diesel blends in a diesel engine. Fuel **2016**, 175, 157–163.

(13) Zhang, Q.; Chen, G.; Zheng, Z.; Liu, H.; Xu, J.; Yao, M. Combustion and emissions of 2,5-dimethylfuran addition on a diesel engine with low temperature combustion. Fuel **2013**, 103, 730–735.

(14) Sirignano, M.; Conturso, M.; D'Anna, A. Effect of furanic biofuels on particle formation in premixed ethylene-air flames: an experimental study. Fuel **2016**, 175, 137–145.

(15) Gogoi, B.; Raj, A.; Alrefaai, M.M.; Stephen, S.; Anjana, T.; Pillai, V.; Bojanampati, S. Effects of 2,5-dimethylfuran addition to diesel on soot nanostructures and reactivity, Fuel **2015**, 159, 766–775.

(16) Esarte, C.; Peg, M.; Ruiz, M.P.; Millera, Á.; Bilbao R.; Alzueta, M.U. Pyrolysis of ethanol: gas and soot products formed. Ind. Eng. Chem. Res. **2011**, 50, 4412–4419.

(17) Ghiassi, H.; Toth, P.; Lighty, J.S. Sooting behaviors of n-butanol and n-dodecane blends. Combust. Flame **2014**, 161, 671–679.

(18) Ruiz, M.P.; Guzmán de Villoria, R.; Millera, Á.; Alzueta, M.U.; Bilbao, R. Influence of different operation conditions on soot formation from C_2H_2 pyrolysis. Ind. Eng. Chem. Res. **2007**, 46, 7550–7560.

(19) Vander Wal, R.L.; Tomasek, A.J. Soot oxidation: dependence upon initial nanostructure. Combust. Flame **2003**, 134, 1–9.

(20) Vander Wal, R.L.; Tomasek, A.J. Soot nanostructure: dependence upon synthesis conditions. Combust. Flame **2004**, 136, 129–140.

(21) Bagi, S.; Sharma, V.; Patel, M.; Aswath, P.B. Effects of diesel soot composition and accumulated vehicle mileage on soot oxidation characteristics. Energy Fuels **2016**, 30, 8479–8490.

(22) Ess, M.N.; Bladt, H.; Mühlbauer, W.; Seher, S.I.; Zöllner, C.; Lorenz, S.; Brüggemann, D.; Nieken, U.; Ivleva, N.P.; Niessner, R. Reactivity and structure of soot generated at varying biofuel content and engine operating parameters. Combust. Flame **2016**, 163, 157–169.

(23) Li, X.; Xu, Z.; Guan, C.; Huang, Z. Impact of exhaust gas recirculation (EGR) on soot reactivity from a diesel engine operating at high load. Appl. Therm. Eng. **2014**, 68, 100–106.

(24) Seong, H.J.; Boehman, A. Impact of intake oxygen enrichment on oxidative reactivity and properties of diesel soot. Energy Fuels **2011**, 25, 602–616.

(25) Yehliu, K.; Vander Wal, R.L.; Armas, O.; Boehman, A.L. Impact of fuel formulation on the nanostructure and reactivity of diesel soot. Combust. Flame **2012**, 159, 3597–3606.

(26) Yehliu, K.; Armas, O.; Vander Wal, R.L.; Boehman, A.L. Impact of engine operating modes and combustion phasing on the reactivity of diesel soot. Combust. Flame **2013**, 160, 682–691.

(27) Arnal, C. Study of reactivity in several environments and characterization of different kinds of diesel soot surrogates. PhD Thesis, University of Zaragoza, Spain 2013.

(28) Guerrero, M.; Ruiz, M.P.; Millera, Á.; Alzueta, M.U.; Bilbao, R. Characterization of biomass chars formed under different devolatilization conditions: differences between rice husk and eucalyptus. Energy Fuels **2008**, 22, 1275–1284.

(29) Mendiara, T.; Alzueta, M.U.; Millera, Á.; Bilbao, R. A comparison of acetylene soot and two different carbon blacks: Reactivity to oxygen and NO. Int. J. Chem. React. Eng. **2007**, 5, A100.

(30) Ruiz, M.P.; Callejas, A.; Millera, Á.; Alzueta, M.U.; Bilbao, R. Soot formation from C_2H_2 and C_2H_4 pyrolysis at different temperatures. J. Anal. Appl. Pyrolysis **2007**, 79, 244–251.

(31) Mendiara, T.; Alzueta, M.U.; Millera, Á.; Bilbao, R. Oxidation of acetylene soot: influence of oxygen concentration. Energy Fuels **2007**, 21, 3208–3215.

(32) Alexandrino, K.; Salinas, J.; Millera, Á.; Bilbao, R.; Alzueta, M.U. Sooting propensity of dimethyl carbonate, soot reactivity and characterization. Fuel **2016**, 183, 64–72.

(33) Alexandrino, K.; Millera, Á.; Bilbao, R.; Alzueta, M.U. Gas and soot formed in the dimethoxymethane pyrolysis. Soot characterization. Fuel Process. Technol. **2018**, 179, 369-377.

(34) Abián, M. Pollutant reduction in combustion systems through flue gas recirculation (FGR). PhD Thesis, University of Zaragoza, Spain 2013.

(35) Stanmore, B.R.; Brilhac, J.F.; Gilot, P. The oxidation of soot: a review of experiments, mechanisms and models. Carbon **2001,** 39, 2247–2268.

(36) Jaramillo, I.C.; Gaddam, C.K.; Vander Wal, R.L.; Lighty, J.S. Effect of nanostructure, oxidative pressure and extent of oxidation on model carbon reactivity. Combust. Flame **2015**, 162, 1848–1856.

(37) Pahalagedara, L.; Sharma, H.; Kuo, C.-H.; Dharmarathna, S.; Joshi, A.; Suib, S.L.; Mhadeshwar, A.B. Structure and oxidation activity correlations for carbon blacks and diesel soot. Energy Fuels **2012**, 26, 6757–6764.

(38) Sharma, H.N.; Pahalagedara, L.; Joshi, A.; Suib, S.L.; Mhadeshwar, B. Experimental study of carbon black and diesel engine soot oxidation kinetics using thermogravimetric analysis, Energy Fuels **2012**, 26, 5613–5625.

(39) Lu, L.; Sahajwalla, V.; Kong, C.; Harris, D. Quantitative X-ray diffraction analysis and its application to various coals. Carbon **2013**, 9, 1821–1833.

(40) Guerrero Peña, G.D.J.; Raj, A.; Stephen, S.; Anjana, T.; Said Hammid, Y.A.; Brito, J.L.; Shoaibi, AA. Physicochemical properties of soot generated from toluene diffusion flames: effects of fuel flow rate. Combust. Flame **2017**, 178, 286–296.

(41) Yen, T.F.; Erdman, G.; Pollack, S.S. Investigation of the structure of petroleum asphaltenes by X-Ray diffraction. Anal. Chem. **1961**, 33, 1587–1594.

(42) Hussain, R.; Mohammad, D. X-ray crystallinity studies of palladium polyacrylate. J. Mater Sci. Technol. **1995**, 11, 310–312.

(43) Al-Qurashi, K.; Boehman, A.L. Impact of exhaust gas recirculation (EGR) on the oxidative reactivity of diesel engine soot. Combust. Flame **2008**, 155, 675–695.

(44) Sadezky, A.; Muckenhuber, H.; Grothe, H.; Niessner, R.; Poschl, U. Raman microspectroscopy of soot and related carbonaceous materials: spectral analysis and structural information. Carbon **2005**, 43, 1731–1742.

(45) Carpentier, Y.; Feraud, G.; Dartois, E.; Brunetto, R.; Charon, E.; Cao, A.-T.; d'Hendecourt, L.; Brechignac, Ph.; Rouzaud, J.-N.; Pino, T. Nanostructuration of carbonaceous dust as seen through the position of the 6.2 and 7.7 µm AIBs. Astron Astrophys **2012,** 548, A40.

(46) Catelani, T.; Pratesi, G.; Zoppi, M. Raman characterization of ambient airborne soot and associated mineral phases. Aerosol Sci. Technol. **2014**, 48, 13–21.

(47) Parent, P.; Laffon, C.; Marhaba, I.; Ferry, D.; Regier, T.Z.; Ortega, I.K.; Chazallon, B.; Carpentier, Y.; Focsa, C. Nanoscale characterization of aircraft soot: a high-resolution transmission electron microscopy, Raman spectroscopy, X-ray photoelectron and near-edge X-ray absorption spectroscopy study. Carbon **2016**, 101, 86–100.

(48) Schmid, J.; Grob, B.; Niessner, R.; Ivleva, N.P. Multiwavelength Raman microspectroscopy for rapid prediction of soot oxidation reactivity. Anal. Chem. **2011**, 83, 1173–1179.

(49) Ivleva, N.P.; McKeon, U.; Niessner, R.; Poschl, U. Raman microspectroscopic analysis of size- resolved atmospheric aerosol particle samples collected with an ELPI: soot, humic-like substances, and inorganic compounds. Aerosol Sci. Technol. **2007**, 41, 655–671.

(50) Dippel, B.; Jander, H.; Heintzenberg, J. NIR FT Raman spectroscopic study of flame soot. Phys. Chem. Chem. Phys. **1999,** 1, 4707–4712.

(51) Hayashida, K.; Nagaoka, H.; Ishitani, H. Growth and oxidation of graphitic crystallites in soot particles within a laminar diffusion flame. Fuel **2014**, 128, 148–154.